Bosch Carbon Catalyst Regeneration in Water II: Analysis of Bosch Catalyst Beads Throughout the Initial Regeneration Process

Eva Swalley[1] and Kathryn Ollenburg[2]
Amentum ASED, Huntsville, AL, 35806

Benjamin Rupp[3] and Ellen Rabenberg[4]
NASA Marshall Space Flight Center, Huntsville AL, 35812

Catalyst integrity is an important factor in reactor longevity since it changes the effectiveness of a reaction. A Carbon Formation Reactor (CFR), used within Series Bosch (S-Bosch), utilizes an iron alloy catalyst to convert carbon monoxide and hydrogen into water and solid carbon. The catalyst promotes the formation of carbon to such an extent that pressure-causing clogs form within the reactor and reaction sites on the catalyst become limited. To remove carbon from both the reactor and the surface of the iron alloy catalyst, a technique was developed that utilizes water, an In-Situ Resource Utilization (ISRU) Resource, and agitation to regenerate the reactor. To ascertain catalyst integrity throughout this regenerative process, sample catalyst beads were taken before and after the carbon formation reaction, and then after the regeneration process. Additionally, wastewater from the regeneration process was sampled. The sampled beads and wastewater were observed under a Scanning Electron Microscopy (SEM) microscope and the beads were chemically etched to determine if the catalyst had degraded at any point during this process, and if catalyst was lost. Minimal catalyst degradation was observed after carbon formation in the CFR.

Acronyms and Nomenclature

AR	=	Air Revitalization
BSE	=	Backscatter Electron
CFR	=	Carbon Formation Reactor
CHX	=	Condensing Heat Exchanger
COR-CaTS	=	Carbon Dioxide Reduction Catalyst Test Stand
DI	=	Deionized
ECLSS	=	Environmental Controls and Life Support Systems
EDS	=	Energy Dispersive X-Ray Spectroscopy
ISRU	=	In-Situ Resource Utilization
ISS	=	International Space Station
LEO	=	Lower Earth Orbit
PIG	=	Pipeline Inspection Gage
RWGS	=	Reverse Water Gas Shift
RWGSR	=	Reverse Water Gas Shift Reactor
S-Bosch	=	Series Bosch
SE	=	Secondary Electron
SEM	=	Scanning Electron Microscopy
WPA	=	Water Processing Assembly

[1] Test Engineer, ECLSS Development Branch, ES62: ECLSS Test Branch, Mail Stop: ES62, MSFC, AL 35812.
[2] Project Lead, ECLSS Development Branch, ES62: ECLSS Test Branch, Mail Stop: ES62, MSFC, AL 35812.
[3] Aerospace Materials Engineer, EM31: Materials Science and Metallurgy Branch, Mail Stop: EM31, MSFC, AL 35812.
[4] Aerospace Materials Engineer, EM31: Materials Science and Metallurgy Branch, Mail Stop: EM31, MSFC, AL 35812.

I. Introduction

DEVELOPING a closed loop Atmospheric Revitalization (AR) system is essential to furthering humanity's reach into the universe. The AR system contains the functions of trace contaminate control, carbon dioxide removal, and oxygen regeneration. The oxygen regeneration device that has operated on the ISS is the Sabatier reactor. Within the Sabatier reactor, the Sabatier reaction detailed in Equation 1 converts metabolic carbon dioxide into methane and water. The methane is vented overboard, and the water is sent to the Water Processing Assembly (WPA) to enter the closed water loop [1]. The elements of water are eventually returned to the AR system by the Oxygen Generation Assembly which splits the water into hydrogen which is sent back to the reactor and oxygen which is sent to the cabin for the crew.

Though the Sabatier reactor does fulfill the role of oxygen regeneration, it requires more functions to be added to the AR architecture to close the loop such as methane post processing and hydrogen purification. If the methane is vented overboard, hydrogen, an essential element of water and the Sabatier reaction, is lost. This loss of hydrogen creates a need for water to be resupplied thus constraining long duration space flight to Low Earth Orbit (LEO) where resupply is sustainable. Methane post processing and hydrogen purification technologies are being investigated [2], [3], [4].

Sabatier Reaction $$CO_2 + 4H_2 \rightleftarrows CH_4 + 2H_2O \quad (1)$$

An alternative solution to close the AR loop is to employ the Bosch process. The Bosch process, detailed in Equations 2 through 4, reacts the metabolic carbon dioxide with hydrogen and outputs solid carbon and water. As such, it doesn't necessitate any further functions since solid-liquid separation methods exist and could be used to deliver the water to the WPA and carbon reuse isn't required for closing the AR loop. Even though Bosch carbon reuse isn't required, it has the potential to be used in In-Situ Resource Utilization (ISRU) projects [5], [6], [7]. The challenges that the Bosch process faced historically were reactor efficiency, catalyst degradation, and over pressurization issues [5], [8], [9], [10], [11].

Reverse Water Gas Shift (RWGS) Reaction $$CO_2 + H_2 \rightleftarrows CO + H_2O \quad (2)$$

CO Hydrogenation Reaction $$CO + H_2 \rightleftarrows C + H_2O \quad (3)$$

Boudouard Reaction $$2CO \rightleftarrows C + CO_2 \quad (4)$$

The reactor efficiency issue was solved through creating two different reactors placed in series since the Reverse Water Gas Shift (RWGS) reaction (Equation 2) and the CO Hydrogenation and Boudouard reactions (Equations 3 and 4) have vastly different reaction kinetics [5]. This led to the creation of Series Bosch (S-Bosch), a combination of reactors and filter membranes seen in Figure 1. The reactor for the RWGS reaction and the two filter membranes have been proven through previous testing. However, the Carbon Formation Reactor (CFR) which houses the Boudouard and CO Hydrogenation reactions (Equations 3 and 4) has yet to be created in a regenerable way even though attempts have been made [5], [8], [9], [10], [11], [12], [13].

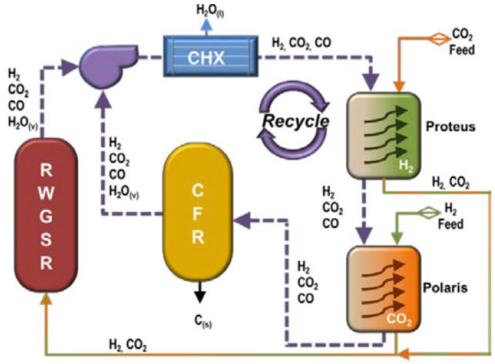

Figure 1. Series Bosch. *A schematic of the S-Bosch test stand consisting of a Reverse Water Gas Shift Reactor (RWGSR), a Carbon Formation Reactor (CFR), the Polaris membrane (depicted in orange), the Proteus membrane (depicted in green), and a Condensing Heat Exchanger (CHX) [9]. The purple symbol in the top left is a pump.*

The CFR is where the catalyst degradation and over pressurization issues occur. The over pressurization issue occurs due to the build-up of elemental carbon in the reactor creating brick-like clogs that historically have had to be mechanically removed from the reactor along with the catalyst [5]. In the other papers in this series, techniques were investigated to break up these clogs and regenerate the surface of the catalyst [14], [15]. These efforts included aggressively washing the catalyst beads in turbulent room temperature water and quenching the beads to thermally shock the catalyst away from the carbon build-up. Results concluded that 10 g of beads could be cleaned from thermal shock and aggressive agitation in thirty minutes thus presenting a solution that could be scaled up and implemented in a reactor [14], [15].

Catalyst degradation is the remaining obstacle for Bosch technology. It is caused by the Boudouard reaction (Equation 3) during carbon formation and is classified as a metal dusting process. Metal dusting is a process where the build-up of carbon on the catalyst forces small flakes of catalyst off its surface to expose more material below. This eventually leads to the entire metal becoming a powdery dust, hence the name. With an iron catalyst, metal dusting eventually stops due to the formation of iron carbides and oxides [16], [17], [18], [19]. This paper will investigate how the beads degraded throughout the initial cleaning process established in the pervious paper in this series to ascertain the severity of catalyst degradation [14].

II. Methods

The Boudouard and CO Hydrogenation reactions took place in the Carbon Dioxide Reduction Catalyst Test Stand (COR-CaTS) with Amasteel S660 Cast Steel Shot as the catalyst. The resulting carbon and catalyst mixture was removed and agitated in room temperature water in previous carbon removal experiments [14]. A sample was taken of unreacted catalyst beads, reacted material from COR-CaTS, and reacted material that had been repeatedly washed until minimal carbon was visibly present in the wastewater. The samples were prepped for optical and Scanning Electron Microscopy (SEM) analysis. The wastewater used in the washing experiments was set aside and prepped for optical and SEM analysis to observe if traces of the iron catalyst were present which would indicate metal dusting.

A. Bead Analysis

Each set of catalyst bead samples were observed and compared to gauge the severity of catalyst degradation that occurs during the carbon formation reaction process. Special care was taken to note the physical conditions and material composition of each catalyst sample set. Both the catalyst sample surface and cross-section were observed in this way.

1. Puck Formation

Each set of catalyst bead samples were mounted in an epoxy puck for optical and SEM analysis. The catalyst beads were placed in a rubber mold that was then filled with a two-part epoxy resin. The mold was then placed under a light vacuum to remove any bubbles that had formed before the epoxy was fully set. For cross-sectional analysis each hardened puck was then ground to reveal a cross-section of the beads and polished to a 1 μm finish.

2. Optical Analysis

Catalyst samples mounted in the epoxy pucks were examined and imaged at various magnifications on a Leica DMi 8 optical microscope. All images and observations were performed under brightfield conditions on the microscope. Chemically etched catalyst sample epoxy pucks were optically examined in the same fashion with the same conditions.

3. Scanning Electron Microscopy (SEM)

Before catalyst bead samples were mounted in epoxy pucks a small portion of each sample grouping was set aside for SEM surface imaging. The samples were fixed in place with carbon tape to the sample holder of a Hitachi S-3700N SEM microscope. Other than the use of the carbon tape to minimize local charging, no changes or alterations, such as sputtering or additional coatings, were made to the samples. Depending on the degree of surface oxidation and surface charging, variable pressures and vacuum modes were used while examining the samples. Backscatter Electron (BSE) and Secondary Electron (SE) imaging were used to further examine the surface texture and underlying varying composition of the catalyst samples at an accelerated voltage of 8 kV. False color mapping of the overall composition of the catalyst samples was generated using Energy-Dispersive X-Ray Spectroscopy (EDS).

The epoxy puck mounted catalyst samples (Section A.1) were affixed to the Hitachi S-3700N SEM microscope using mount holders and setscrews. BSE imaging while under variable pressure mode at an accelerated voltage of 8 kV was used to analyze the epoxy materials in order to account for the resin material and the potential of charging on the samples. In order to achieve optimum EDS mapping and line scanning for the material composition of the catalyst samples, the accelerating voltage was set to 15 kV.

4. Chemical Etching

The catalyst samples mounted on the epoxy pucks (Section A.1) were then ground again and polished to a 0.5 µm finish to remove any oxides that had formed during previous SEM analysis as described in Section A.3. After polishing, the pucks were etched with 2% Nital to further examine the grain structure of the catalyst beads. After etching, the pucks were optically analyzed as described in Section A.2.

B. Wastewater Analysis

During the previously reported experiments, wastewater from the regeneration process was collected and set aside in bottles [14]. Samples of the wastewater were taken and observed optically and with SEM to confirm metal dusting.

1. Optical Analysis

A plastic pipette was used to take a sample of the wastewater which was then deposited on a Fisherbrand Superfrost® microscope slide. The slide was then placed on an Olympus SZX-ILLD100 Optical Microscope. The microscope magnification was adjusted until the sample was visible. Images of the catalyst particles were taken using a phone camera rig affixed to the microscope eyepiece as well as a QImaging Retiga R6 camera attachment on the microscope.

2. Scanning Electron Microscopy (SEM)

A plastic pipette was used to obtain a sample of the sediment from a wastewater bottle. The sample was placed on an aluminum stub with carbon tape that can be affixed to the SEM microscope. Before imaging, the sample was placed in a desiccator for a few days to dry out completely. SE and BSE images were taken using a FEI Quanta 600F Environmental SEM microscope to observe the material layering, and the composition of the sample was determined with the Oxford Instruments X-MaxN 80 EDS detector on the microscope. SEM images were taken under a high vacuum and the accelerating voltage was set to 15 kV.

III. Observations and Discussion

The catalyst beads appear to degrade minimally over the course of the carbon formation reaction process. During the carbon formation reaction process, carbon displaces iron catalyst particles as it forms on the catalyst surface. These catalyst particles are enmeshed in the carbon soot that forms in the reactor. Samples of the carbon-coated catalyst that were repeatedly washed in previous experiments became slightly warped. Additionally, agitation of the beads may have abraded the cracks and pitting that occurred on the surface during the reaction process. Catalyst particles that were trapped in carbon soot were found in the regeneration wastewater. Figures beginning with A are in the Appendix.

A. Bead Analysis

1. Optical Analysis

The sample cross-sections of unreacted catalyst, carbon-coated catalyst from the COR-CaTs reactor, and carbon-coated catalyst that had been washed repeatedly until minimal visible carbon was present on the catalyst surface were optically analyzed. All samples observed were highly porous and contained dendritic regions under the bead surface along the edges as well as within the center of the beads. Additionally, some bead samples contained void spaces. These characteristics are the result of the controlled atomization process employed by the catalyst manufacturer.

Cross-sections of the unreacted catalyst show that the outer edges of the beads contain minor imperfections such as crevices and pits. After etching the cross-sections, it was observed that the outer edge of the beads was oxidized and that surrounding the interior voids were small dendritic regions. Chemical etching also showed that the metal structure of the beads was tempered martensite/bainite. Images of the cross-sectional analysis of the unreacted catalyst are displayed in Figure 2.

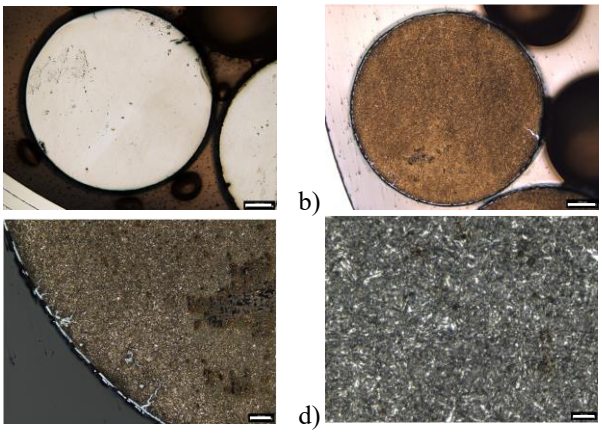

Figure 2. Unreacted Catalyst Bead Cross-Sectional Images. *All images were taken using an optical microscope. a) Image of the cross-section at a magnification of 50x with a 250 µm scale bar. b) Image of the cross-section etched in 2% Nital at a magnification of 50x with a 250 µm scale bar. c) Image of the edge of the cross-section etched in 2% Nital at a magnification of 200x with a 50 µm scale bar. d) Image of the center of the cross-section etched in 2% Nital at a magnification of 1000x with a 10 µm scale bar.*

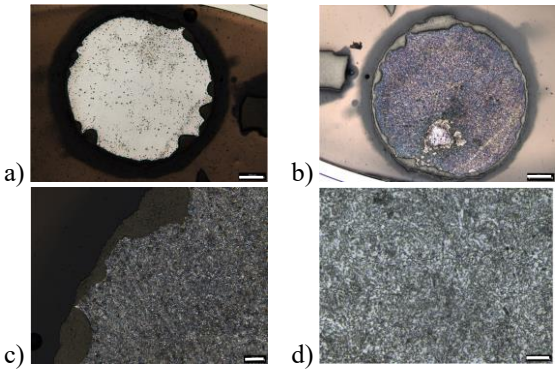

Figure 3. Carbon-Coated Catalyst Bead Cross-Sectional Images. *All images were taken using an optical microscope. a) Image of the cross-section at a magnification of 50x with a 250 µm scale bar. b) Image of the cross-section etched in 2% Nital at a magnification of 50x with a 250 µm scale bar. c) Image of the edge of cross-section etched in 2% Nital at a magnification of 200x with a 50 µm scale bar. d) Image of the cross-section center etched in 2% Nital at a magnification of 1000x with a 25 µm scale bar.*

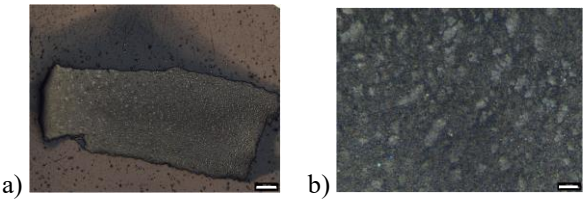

Figure 4. Carbon-Coated Catalyst Bead Cross-Sectional Images. *All images were taken using an optical microscope. a) Image of the cross-section at a magnification of 100x with a 100 µm scale bar. b) Image of the cross-section at magnification of 1000x with a 10 µm scale bar.*

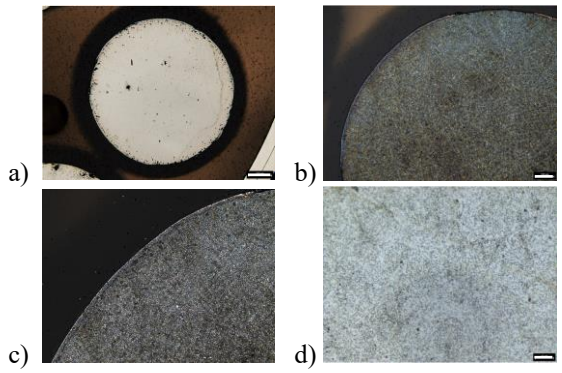

Figure 5. Repeatedly Washed Carbon-Coated Catalyst Bead Cross-Sectional Images. *All images were taken using an optical microscope. a) Image of the cross-section at a magnification of 50x with a 250 µm scale bar. b) Image of the cross-section etched in 2% Nital at a magnification of 100x with a 100 µm scale bar. c) Image of the cross-section edge etched in 2% Nital at a magnification of 200x. d) Image of the cross-section center etched in 2% Nital at a magnification of 1000x with a 10 µm scale bar.*

The observation of the carbon-coated catalyst revealed deep pits that were full of carbon and carbon deposits found deeper under the surface of the bead as is shown in SEM images of the cross-section in Figure A4. This is due to the displacement of iron caused by the Boudouard reaction and the porous nature of the catalyst beads. The carbon layer thickness ranged from 25 – 150 µm on the surface of the bead. After etching the beads, it was observed that the surface of the beads was no longer oxidized due to the reaction process. Microcracks were observed throughout the carbon-coated bead samples as well as oxidation of the dendritic regions. Additionally, the tempered-martensite/bainite structure of the beads observed in the unreacted catalyst appeared to be transitioning to annealed martensite. Images of the carbon-coated catalyst cross-sectional analysis are displayed in Figure 3.

Within the same puck, containing the carbon-coated catalyst beads, were packed carbon masses. The cross-section of one of these carbon masses revealed small flecks of iron embedded in the mass. This confirms that metal dusting of the catalyst occurs during the carbon formation process. Images of the carbon mass cross-section are displayed in Figure 4.

Carbon-coated catalyst beads that had been washed repeatedly appeared to have traces of pitting and interior carbon deposits that were not as extreme as what was observed in the unwashed carbon-coated catalyst. It is believed that as the catalyst beads were agitated, the impact of the beads against each other and the stir bar abraded the exterior of the beads. Observation of the edge of the bead cross-section after etching showed no visible carbon remaining on the bead surface as a result of the regeneration process. The bead surface is further examined for traces of carbon in Section A.2. The washed catalyst beads have an oxidized exterior similar to that of the unreacted catalyst and retained the oxidation surrounding the dendritic regions that was observed after the carbon formation process. It was observed that no major changes were made to the microstructure of the beads. Images of the cross-sectional analysis of the washed carbon-coated catalyst beads are displayed in Figure 5.

2. Scanning Electron Microscopy (SEM)

SEM images of both the surface and cross-section of samples of unreacted catalyst, carbon-coated catalyst from the COR-CaTs reactor, and carbon-coated catalyst that had been washed repeatedly until minimal visible carbon was present in the wastewater were taken and optically analyzed. The material make-up of the catalyst samples was observed both on the surface and in the cross-section of each catalyst sample. Energy-Dispersive X-Ray Spectroscopy (EDS) line scans were performed on the cross-sections of each of the catalyst samples.

Observation of the surface of the unreacted catalyst beads showed uneven layers of iron oxide that formed in raised sections. Some parts of these layers appeared to have flaked off revealing additional iron oxide beneath the vacant areas. Pores and crevices are also visible on the surface of these samples. SEM images of the surface of the unreacted catalyst are displayed in Figure 6 and images of the material composition of the bead surface are displayed in Figure A1. Further SEM analysis was performed on the cross-sections of the unreacted catalyst beads. The EDS line scans of the beads showed that there were no great quantities of unevenly distributed materials around the dendritic regions of the beads. The line scans also showed a higher concentration of carbon in the exterior portions of the beads. This distribution of carbon is due to the manufacturing process of the catalyst. Images of the cross-sectional analysis of the unreacted catalyst beads are displayed in Figure 7 and images of the cross-section material analysis are displayed in Figure A2.

SEM images were taken of the surface of the carbon-coated catalyst beads, and the images show that the beads are evenly coated in carbon with miniscule specks of the iron bead surface visible. Images of the surface and outer material composition of the carbon-coated catalyst are displayed in Figure 8 and Figure A3. SEM imaging of the bead's cross-section confirmed the displacement of iron as carbon formed during the reaction process as was observed under the optical microscope in Section A.1. EDS line scans of the bead's cross-section showed spikes of carbon in deposits within the interior of the beads, particularly around the dendritic regions where the beads are more porous. Despite the pitting noted on the bead's surface, the majority of the catalyst bead appears to remain viable. The oxide layer observed on the surface of the unreacted beads was not present on the surface of the carbon-coated beads. This indicates that the oxide layer on the bead's surface is removed during the carbon formation reaction. Oxidation around the dendritic regions was observed in imaging and line scans. Images of the carbon-coated catalyst bead's cross-section are displayed in Figure 9 and images of the cross-section material composition of the catalyst are displayed in Figure A4.

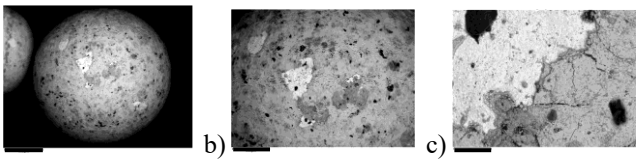

Figure 6. Unreacted Catalyst Bead Surface SEM Images. *All images were taken using Backscatter Electron (BSE) imaging. a) Image of the surface at a magnification of 50x with a 500 µm scale bar* **[14]**. *b) Image of the surface at a magnification of 100x with a 250 µm scale bar. c) Image of the surface at a magnification of 1000x with a 25 µm scale bar.*

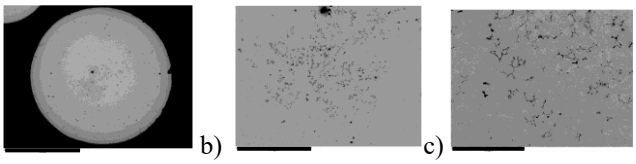

Figure 7. Unreacted Catalyst Bead Cross-section SEM Images. *All images were taken using Backscatter Electron (BSE) imaging. a) Image of the cross-section at a magnification of 50x with a 1 mm scale bar. b) Image of the cross-section center at a magnification of 200x with a 250 µm scale bar. c) Image of the cross-section center at a magnification of 500x with a 100 µm scale bar.*

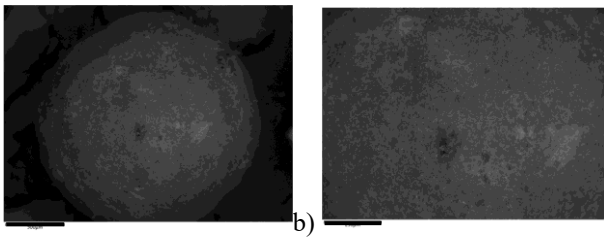

Figure 8. Carbon-Coated Catalyst Bead Surface SEM Images. *All images were taken using Backscatter Electron (BSE) imaging. a) Image of the surface at a magnification of 50x with a 500 µm scale bar* **[14]**. *b) Image of the surface at a magnification of 100x with a 250 µm scale bar.*

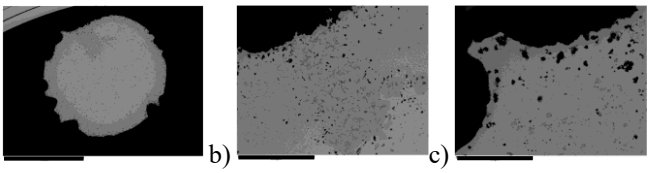

Figure 9. Carbon-Coated Catalyst Bead Cross-Section SEM Images. *All images were taken using Backscatter Electron (BSE) imaging. a) Image of the cross-section at a magnification of 50x with a 1 mm scale bar. b) Image of the cross-section at a magnification of 200x with a 250 µm scale bar. c) Image of the cross-section at a magnification of 500x with a 100 µm scale bar.*

Analysis of the surface of the carbon-coated beads that had been repeatedly washed showed that the beads were slightly warped. This is likely due to either the agitation of the washing process or the catalyst degradation that occurs during the carbon formation reaction. The surface of the washed catalyst beads appeared to be rough with small pockets and crevices. Small patches of remaining carbon are littered across the surface of the beads, and the remaining bead surface is comprised of iron/iron-oxide. The SEM images of the surface of the beads are displayed in Figure 10 and the images of the material composition of the surface of the beads are displayed in Figure A5. Images of the cross-section of the washed beads showed similar characteristics to that of the interior of the unwashed carbon-coated beads. Pockets of carbon were observed under the surface of the beads and around dendritic regions. EDS line scans showed oxidation around the dendritic regions which remained from the unwashed carbon-coated catalyst beads. Carbon deposits located within the bead interior are due to the porosity of the bead material used within the reaction process. SEM images of the cross-section of the repeatedly washed catalyst beads are displayed in Figure 11 and images of the material composition of the cross-section of the beads are displayed in Figure A6.

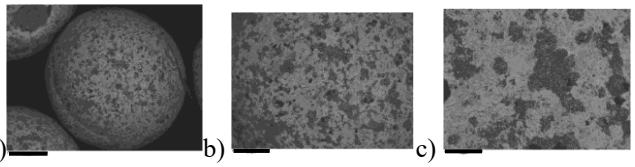

Figure 10. Repeatedly Washed Carbon-Coated Catalyst Bead Surface SEM Images. *All images were taken using Backscatter Electron (BSE) imaging. a) Image of the surface at a magnification of 50x with a 500 µm scale bar* **[14]**. *b) Image of the surface at a magnification of 100x with a 250 µm scale bar. c) Image of the surface at a magnification of 500x with a 50 µm scale bar.*

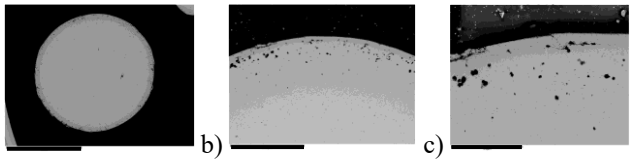

Figure 11. Repeatedly Washed Carbon-Coated Catalyst Bead Cross-Section SEM Images. *All images were taken using Backscatter Electron (BSE) imaging. a) Image of the cross-section at a magnification of 50x with a 1 mm scale bar. b) Image of the cross-section at a magnification of 200x with a 250 µm scale bar. c) Image of the cross-section at a magnification of 500x with a 100 µm scale bar.*

B. Wastewater Analysis

1. Optical Analysis

A sample of the wastewater from carbon-coated catalyst experiments was observed under an optical microscope. Under the microscope, small shiny particles were observed. These particles are most likely catalyst bead fragments that were displaced either during the carbon formation process or during the regeneration process. Images of the particles are displayed in Figure 12.

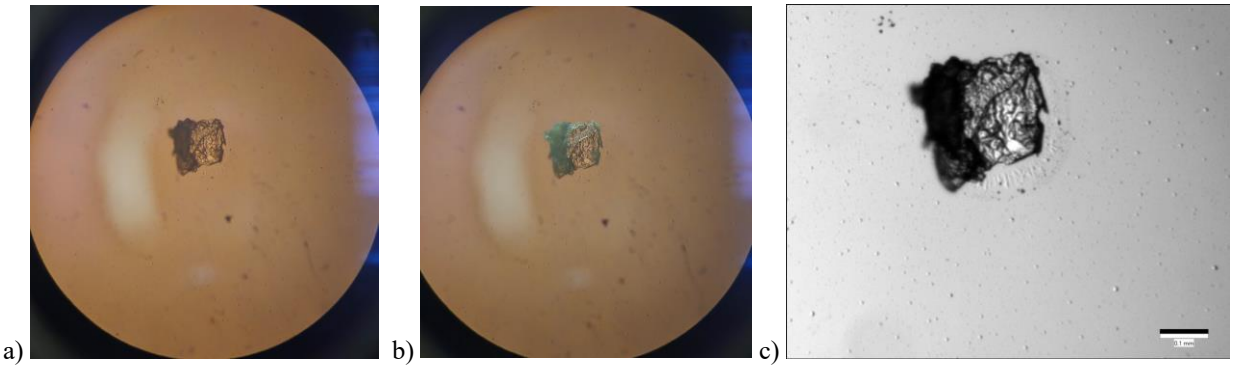

Figure 12. Iron Catalyst Particle Sample Images from Carbon-Coated Bead Washing Experiments. *Images a)-b) were taken using a phone camera viewing port on the microscope. Image c) was taken using the optical microscope software. a) Image of a catalyst particle found in wastewater bottle. b) Image of light reflecting off of the catalyst particle. c) Image of the catalyst particle with scale bar at 0.1 mm.*

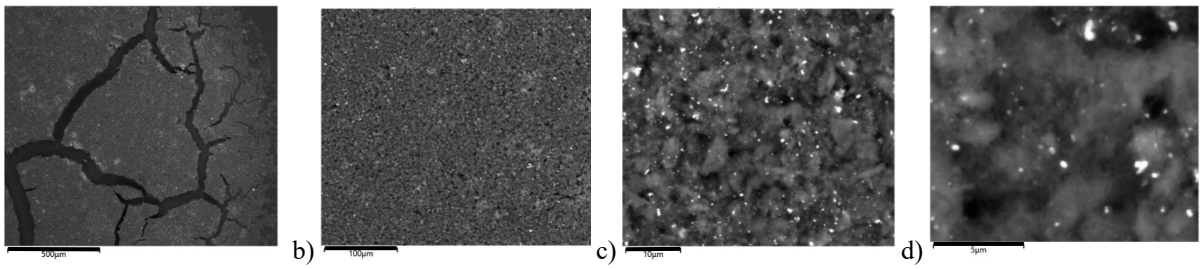

Figure 13. Iron Catalyst and Carbon Wastewater Sample SEM Images from Carbon-Coated Bead Washing Experiments. *All images were taken using Backscatter Electron (BSE) imaging. a) Image of sediment at a magnification of 100x with a 500 µm scale bar. b) Image of sediment at a magnification of 400x with a 100 µm scale bar. c) Image of sediment at a magnification of 3000x with a 10 µm scale bar. d) Image of sediment at a magnification of 10000x with a 5 µm scale bar.*

2. Scanning Electron Microscopy (SEM)

A sample of carbon and catalyst particles that collected at the bottom of a wastewater bottle was taken for SEM analysis. SEM images show a dried out, cracked layer of carbon with miniscule flakes of iron catalyst interspersed amongst the carbon. Material composition scans of the sample also confirm the presence of iron catalyst particles. Additionally, the iron deposits within the carbon are highly oxidized. The presence of the iron deposits enmeshed in the carbon within the wastewater sediment confirms that metal dusting occurs during the carbon formation reaction. Images of the sample are displayed in Figure 13 and material composition images of the sample are displayed in Figure A7.

IV. Conclusion and Future Work

SEM imaging revealed that the unreacted catalyst beads are oxidized before placement in the CFR, but this does not affect the ability of carbon to form on the surface of the beads. Microscope images of the catalyst beads throughout the regeneration process show that while there is catalyst degradation in the form of metal dusting, the majority of the catalyst material remains. This indicates that a cyclical process utilizing the regeneration techniques developed in the first paper in this series is possible [14]. Regenerating the carbon-coated catalyst beads' surface leaves behind trace amounts of carbon, but the bead surface is still able to oxidize indicating available activation sites. The observations made on the catalyst integrity as well as the findings detailed in the first paper of this series lead us to conclude that regenerated beads could be re-reacted successfully in a CFR. Catalyst degradation was minimal enough that the beads could withstand multiple reaction and regeneration cycles. Currently, lab-scale devices are being developed to separate the carbon and water waste stream and to agitate the catalyst within a reactor. These devices will eventually be placed in a four crew member reactor which will undergo cyclical testing.

Appendix

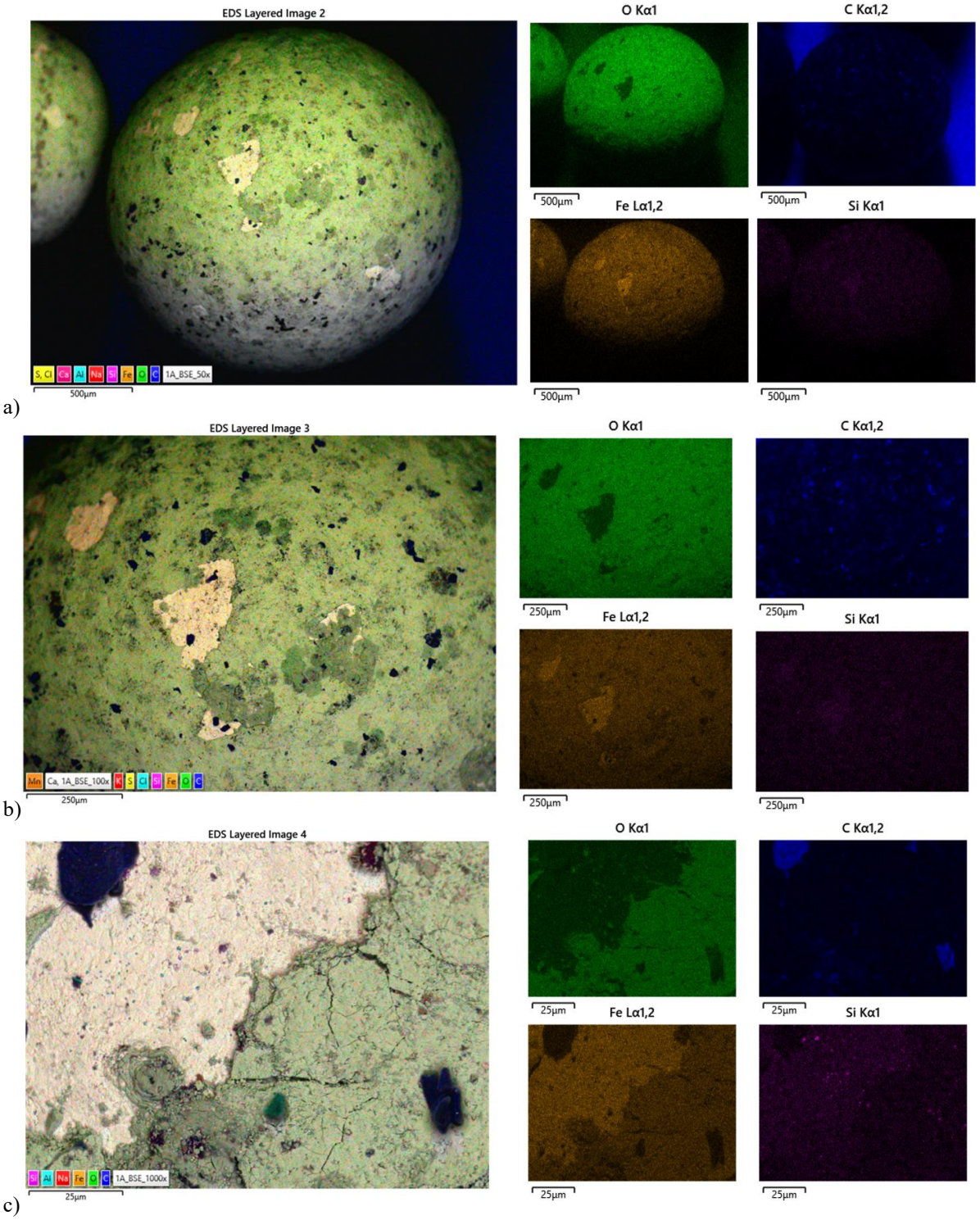

Figure A1. Unreacted Catalyst Bead Surface Material Composition SEM Images. *All images were taken using Backscatter Electron (BSE) imaging. a) Image of the material composition at a magnification of 50x. b) Image of the material composition at a magnification of 100x* **[14]**. *c) Image of the material composition at a magnification of 1000x.*

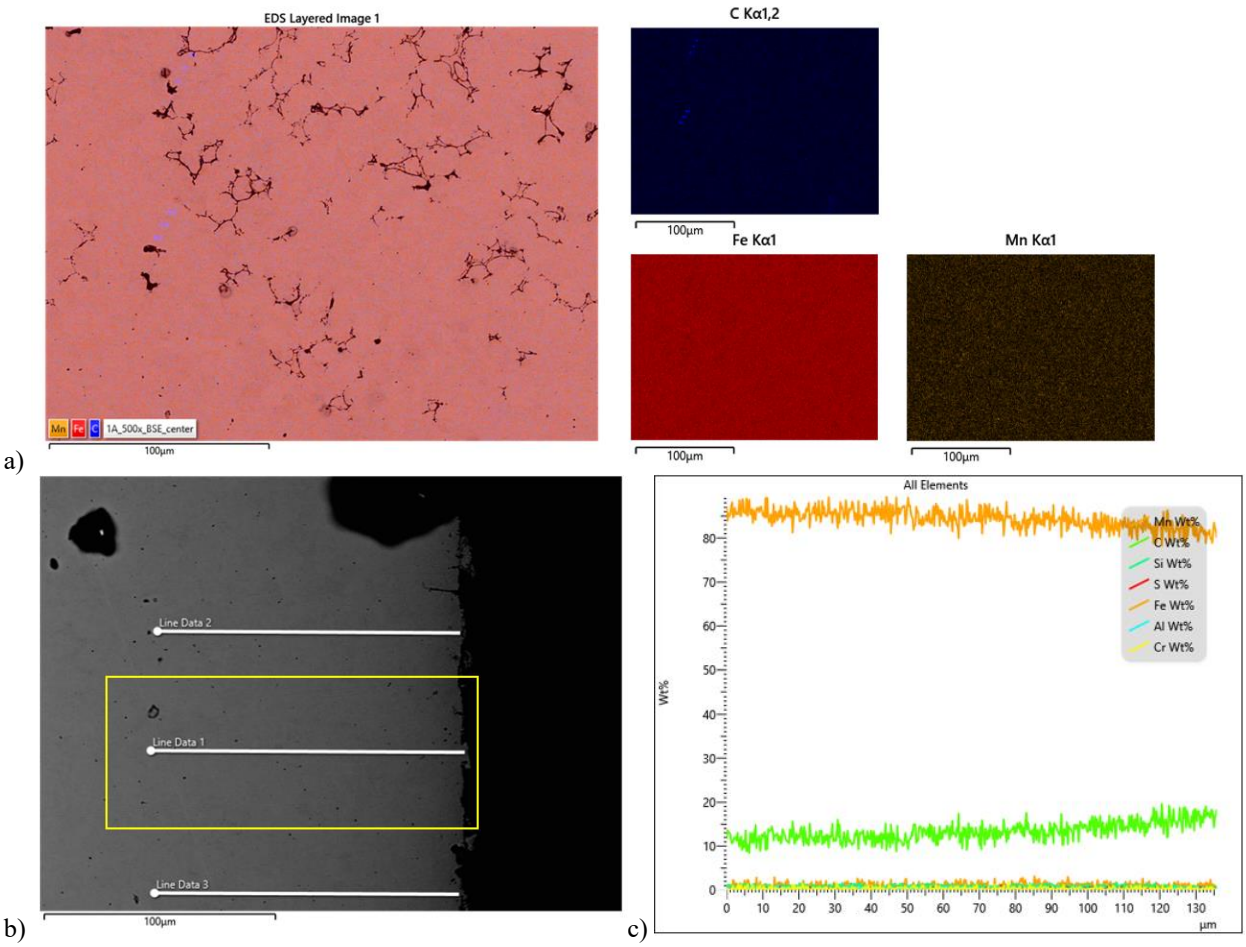

Figure A2. Unreacted Catalyst Bead Cross-Section Material Composition SEM Images. *All images were taken using Backscatter Electron (BSE) imaging. a) Energy-Dispersive X-Ray Spectroscopy (EDS) image of the material composition at a magnification of 500x. b) EDS line scan image of the material composition at a magnification of 500x. c) Graph of weight percentage of materials detected in the ESD line scan from b).*

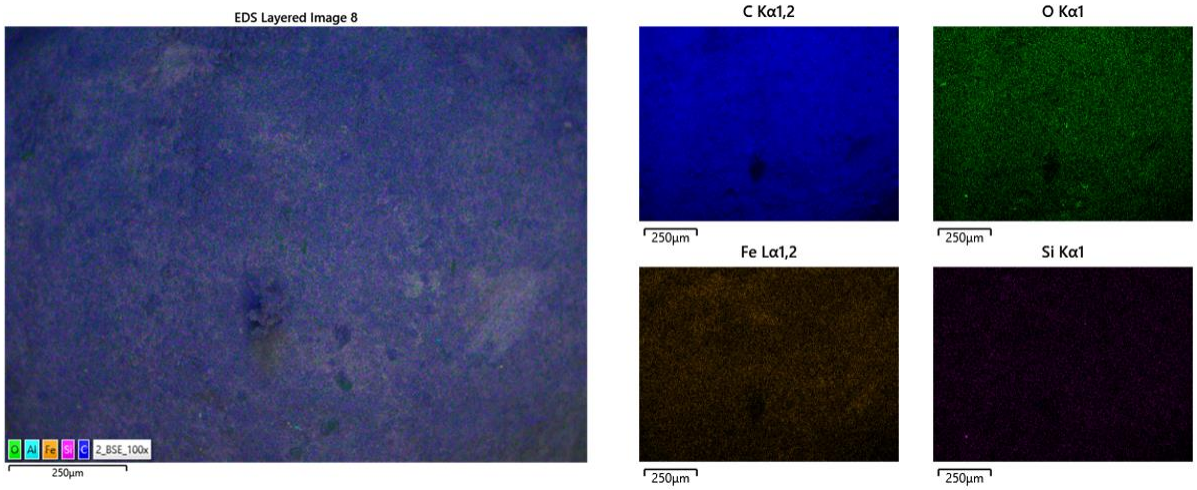

Figure A3. Carbon-Coated Catalyst Bead Surface Material Composition SEM Images. *Image of the material composition of the surface at a magnification of 100x taken using Backscatter Electron (BSE)* **[14]**.

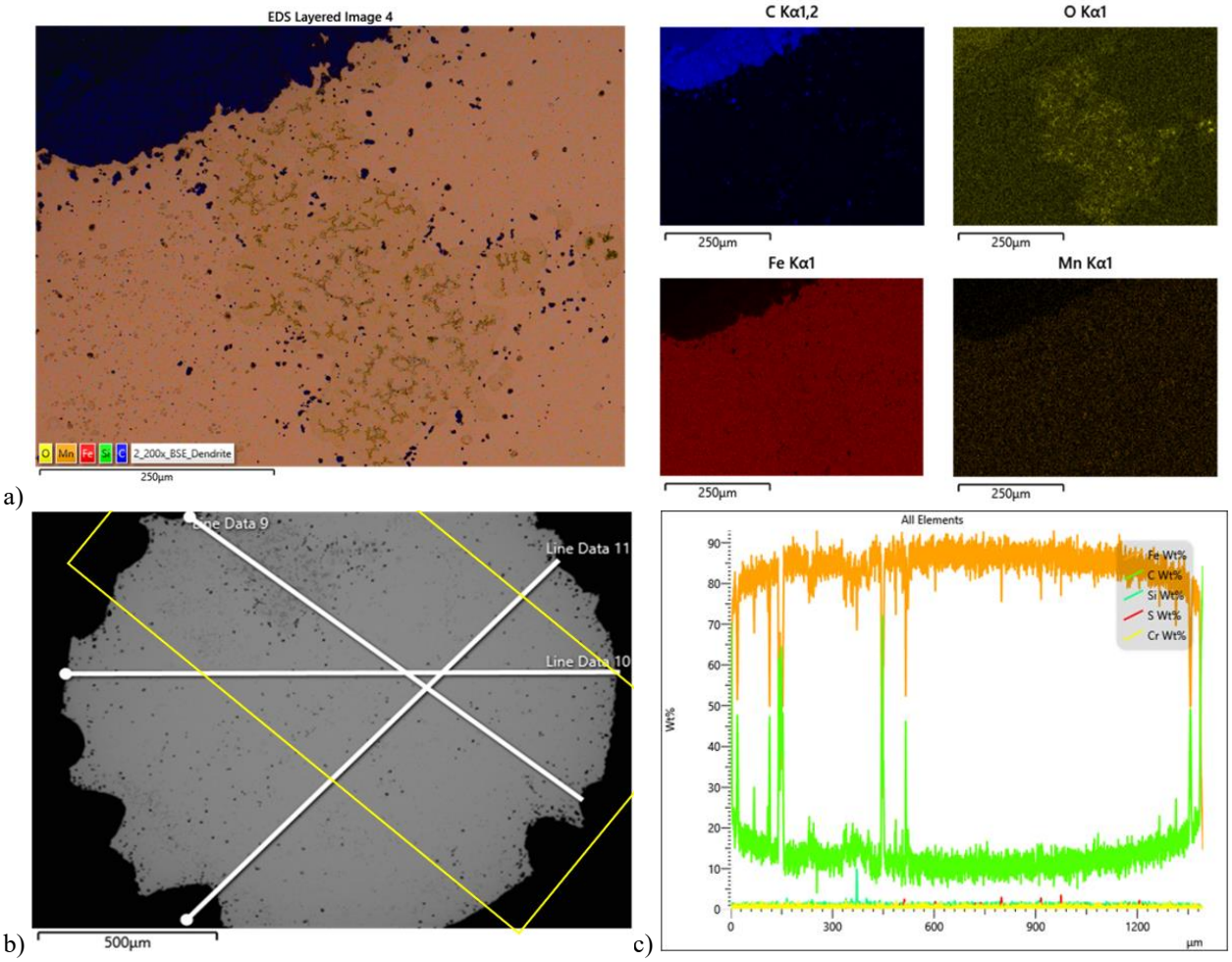

Figure A4. Carbon-Coated Catalyst Bead Cross-Section Material Composition SEM Images. *All images were taken using Backscatter Electron (BSE) imaging. a) Energy-Dispersive X-Ray Spectroscopy (EDS) image of the material composition at a magnification of 200x. b) EDS line scan image of the material composition at a magnification of 75x. c) Graph of weight percentage of materials detected in the ESD line scan from b).*

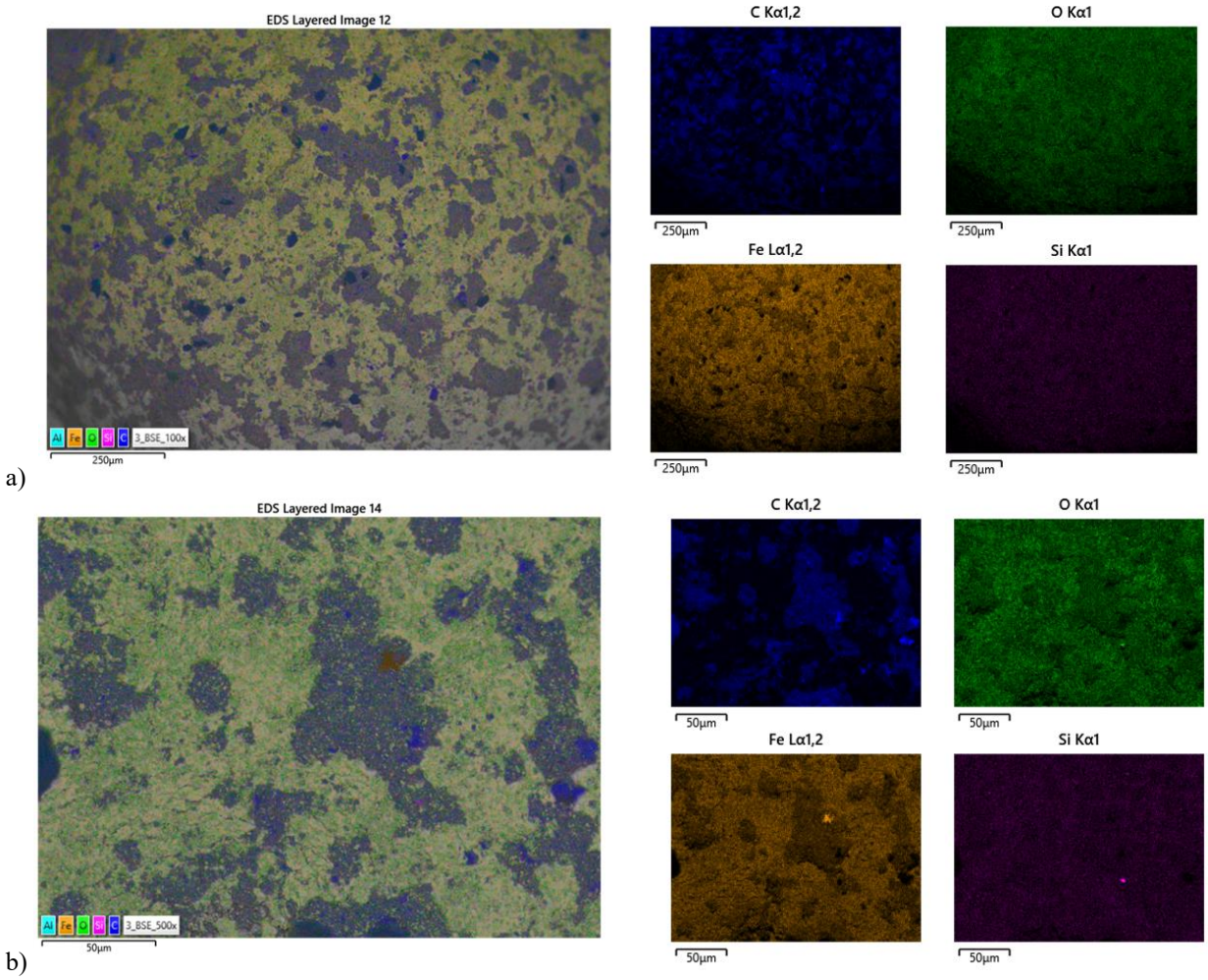

Figure A5. Repeatedly Washed Carbon-Coated Catalyst Bead Surface Material Composition SEM Images. *All images were taken using Backscatter Electron (BSE) imaging. a) Image of the material composition of the surface at a magnification of 100x* **[14]**. *b) Image of the material composition at a magnification of 500x.*

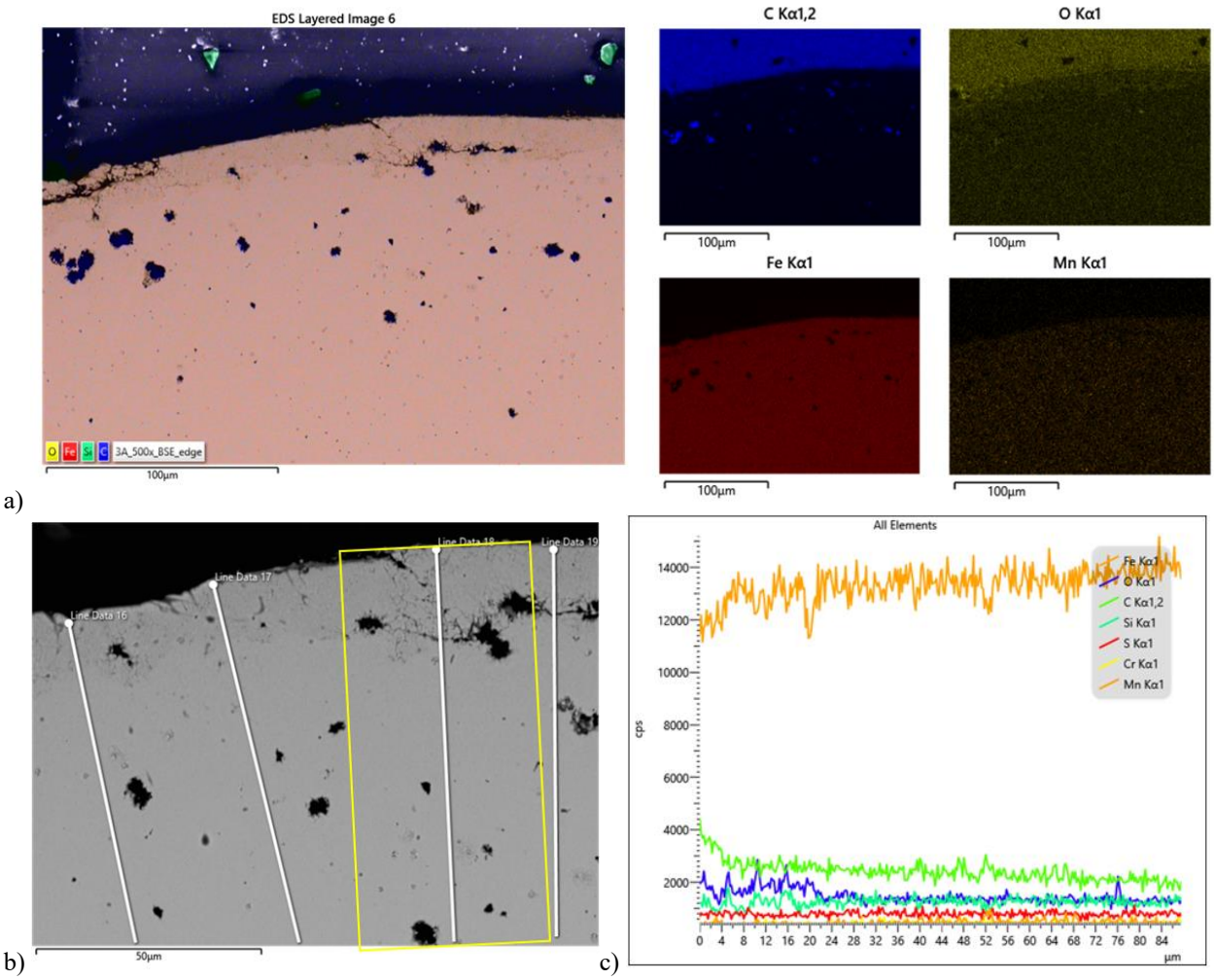

Figure A6. Repeatedly Washed Carbon-Coated Catalyst Bead Cross-Section Material Composition SEM Images. *All images were taken using Backscatter Electron (BSE) imaging. a) Energy-Dispersive X-Ray Spectroscopy (EDS) image of the material composition of the cross-section of a carbon-coated catalyst bead at a magnification of 500x. b) EDS line scan image of the material composition of the cross-section edge of an unreacted catalyst bead at a magnification of 1000x. c) Graph of weight percentage of materials detected in the ESD line scan from b).*

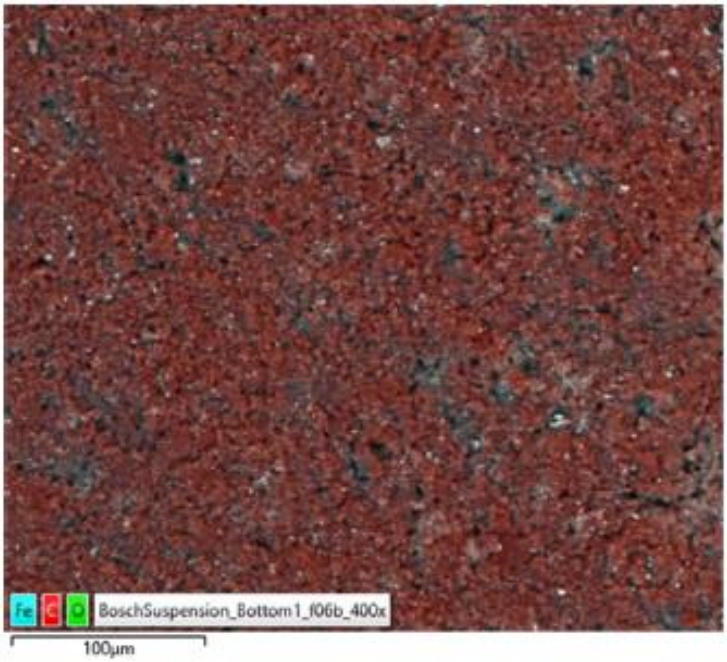

a)

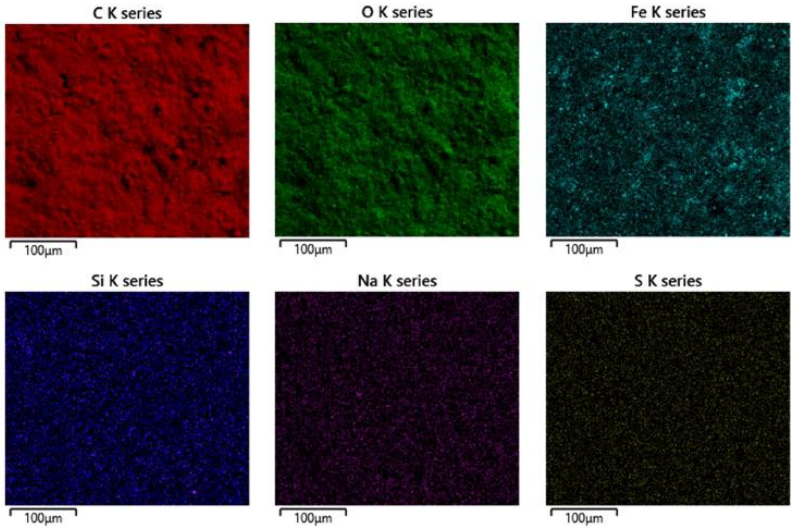

b)

Figure A7. Iron Catalyst and Carbon Wastewater Sample Material Composition SEM Images from Carbon-Coated Bead Washing Experiments. *All images were taken using Backscatter Electron (BSE) imaging. a) Image of the material composition of carbon-coated catalyst washing experiment wastewater sediment at a magnification of 400x. b) Image of the material composition breakdown of the carbon-coated catalyst washing experiment wastewater sediment at a magnification of 400x.*

Acknowledgments

The authors would like to acknowledge Kaitlin Oliver-Butler and Eric Beitle for their assistance in post experiment analysis, editing assistance, and test direction guidance. They would like to acknowledge Tim Giesy and Jeff Mehan for the production and supplication of reacted and unreacted catalyst material used. They would like to acknowledge Chelsea McCool and Stanton Woodard for their assistance with experimentation and laboratory expertise.

References

[1] J. Williamson, J. P. Wilson and H. Luong, "Status of ISS Water Management and Recovery," in *53rd International Conference on Environmental Systems*, Louisville, KY, ICES-2024-317.

[2] K. Crawford, C. S. J. Black and T. Quillin, "Increased Oxygen Recovery Using Plasma Pyrolysis Technology and Electrochemical Hydrogen Separation," in *52nd International Conference on Environmental Systems*, Calgary, Canada, ICES-2023-260, 2023.

[3] A. Childers, M. Triezenberg, S. F. Yates and A. Parsons, "Methane Pyrolysis Enables Closed Loop ECLSS - Progress Report for Advanced Materials Reactor and Advances in Reducing Substrate ESM," in *54th International Conference on Environmental Systems*, Prague, Czech Republic, ICES-2025-394, 2025.

[4] K. Crawford, R. Ozdemir, M. Sansoucie, K. Ollenburg and S. Woodard, "Evaluation of Low-Energy Hydrogen Separation method using Metal-Organic Frameworks (MOFs) for Closed-Loop ECLSS Air Revitalization (CLEAR)," in *55th International Conference on Environmental Systems*, Rio Grande, Puerto Rico, ICES-2026-78, 2026.

[5] Z. W. Greenwood, M. B. Abney, B. R. Brown, E. T. Fox and C. Stanley, "State of NASA Oxygen Recovery," in *48th International Conference on Environmental Systems*, Albuquerque, New Mexico, ICES-2018-48, 2018.

[6] N. W. Wilson, B. Mete, N. J. Payne, J. Tropp and G. G. Botte, "Adaptable Pectin Extraction and Functional Group Impact on Electrolytes Suitable for Energy Storage Applications," *Journal of The Electrochemical Society,* vol. 172, no. 2, p. 023505, 2025.

[7] B. Compton and J. Stewart, "Developments of Bosch Process Architectures for ISRU and Terrestrial Applications," in *European Lunar Symposium 2024*, Dumfries, Scotland, 2024.

[8] M. B. Abney, M. Mansell, B. Barnett, C. M. Stanley, C. Junaedi, S. A. Vilekar and R. Kent, "Demonstration of Robustness and Integrated Operation of a Series-Bosch System," in *46th International Conference on Environmental Systems*, Vienna, Austria, ICES-2016-262, 2016.

[9] C. Stanley, M. B. Abney and B. Barnett, "Evolving Maturation of the Series-Bosch System," in *47th International Conference on Environmental Systems*, Charleston, South Carolina, ICES-2017-219, 2017.

[10] C. Stanley, B. Barnett, P. Matter, M. Beachy, J. Thompson and S. F. Kelly, "Alternative Carbon Formation Reactors for the Series-Bosch System," in *48th International Conference on Environmental Systems*, Albuquerque, New Mexico, ICES-2018-22, 2018.

[11] M. Powell, P. Matter, C. Holt, C. Wiswesser, M. Burke, D. Baumgartner, B. Couch, K. Oberhaus, C. Thompson and M. Holt, "Continued Development of an Automated Carbon Formation Reactor as a Life Support Technologies Solution for Long-Duration Manned Missions and In-Situ Resource Utilization," in *53rd International Conference on Environmental Systems*, Louisville, Kentucky, ICES-2024-68, 2024.

[12] P. E. Hintze, A. C. Muscatello, T. L. Gibson, J. G. Captain, G. M. Lunn, R. W. Devor, B. Bauer and S. Parks, "Self-Cleaning Boudouard Reactor for Full Oxygen Recovery from Carbon Dioxide," in *46th International Conference on Environmental Systems*, Vienna, Austria, ICES-2016-287, 2016.

[13] K. Oliver-Butler and M. Woolever, "Ionic Liquids for a Regenerable Carbon Formation Reactor: Reactor Design Study and Ionic Liquid Parameterization," in *52nd International Conference on Environmental Systems*, Calgary, Canada, ICES-2023-403, 2023.

[14] K. Ollenburg, E. Swalley and B. Rupp, "Bosch Carbon Catalyst Regeneration in Water I: Bosch Carbon Removal from Reacted Beads Utilizing Mechanical Agitation," in *55th International Conference on Environmental Systems*, Rio Grande, Puerto Rico, ICES-2026-242, 2026.

[15] K. Ollenburg, C. Murphy, C. Gordon and E. Swalley, "Bosch Carbon Catalyst Regeneration in Water III: Experiments for and Related to Thermal Shock," in *55th International Conference on Environmental Systems*, Rio Grande, Puerto Rico, ICES-2026-489, 2026.

[16] H. Cheng, D. B. Reiser and S. Dean, "On the mechanism and energetics of Boudouard reaction at FeO (1 0 0) surface: 2CO→C+CO2," *Catalysis Today,* vol. 50, no. 3-4, pp. 579-588, 1999.

[17] P. L. Walker, J. F. Rakszawski and G. R. Imperial, "Carbon Formation from Carbon Monoxide-Hydrogen Mixtures Over Iron Catalysts II. Rates of Carbon Formation," *Journal of Physical Chemistry,* vol. 63, pp. 140-149, 1959.

[18] M. P. Manning, *An Investigation of the Bosch Process,* Massachusetts Institute of Technology Dissertation, 1976.

[19] A. Sacco, *An Investigation of the Reactions of Carbon Dioxide, Carbon Monoxide, Methane, Hydrogen, and Water over Iron, Iron Carbides, and Iron Oxides,* Massachusetts Institute of Technology Dissertation, 1977.